

Structural correlation between Rh–P and Rh–C bond distances vs.
 ^{31}P and ^{13}C NMR parameters in monocarbonylphosphinerhodium(I)
complexes: crystal structure of (methyl
2-(amino)-1-cyclopentene-1-dithio
arboxylato- $\kappa N, \kappa S$)-carbonyl(triphenylphosphine)rhodium(I)¹

Gideon J.J. Steyn^a, Andreas Roodt^{* a}, Irina Poletaeva^b, Yury S. Varshavsky^{b,*}

^a Department of Chemistry, University of the Orange Free State, Bloemfontein 9300, South Africa

^b S.V. Lebedev National Rubber Research Institute, 1 Gapsalskaja str., 198035 St. Petersburg, Russia

Received 13 June 1996; accepted 19 July 1996

Abstract

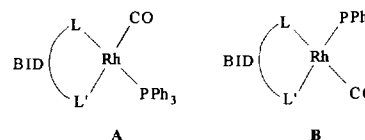
The crystal structure of (methyl 2-(amino)-1-cyclopentene-1-dithiocarboxylato- $\kappa N, \kappa S$)-carbonyl(triphenylphosphine)rhodium(I), $[\text{Rh}(\text{hacsm})(\text{CO})(\text{PPh}_3)]$, was determined. The complex crystallizes in the monoclinic space group $P2_1/c$ with $a = 16.430(1)$, $b = 9.930(1)$, $c = 17.194(1)$ Å, $\beta = 90.72(1)^\circ$, $Z = 4$, $R = 2.89\%$ from refinement of 3143 reflections. The structural data obtained by this study were correlated with ^{31}P and ^{13}C NMR data measured for different $[\text{Rh}(\text{L},\text{L}'\text{-BID})(\text{CO})(\text{PPh}_3)]$ complexes (L,L'-BID = monocharged bidentate ligand with donor atoms L, L': variations of oxygen, nitrogen and sulphur). A good correlation between $^1J(^{31}\text{P}\text{-}^{103}\text{Rh})$ and the Rh–P bond distance was obtained. © 1997 Elsevier Science S.A.

Keywords: Rhodium; Carbonyl; NMR; Crystal; Dithiocarboxylato; Crystal structure

1. Introduction

This crystallographic and NMR study is a part of a continued investigation [1–9] of the ligand effects in square planar $[\text{Rh}(\text{L},\text{L}'\text{-BID})(\text{CO})(\text{PPh}_3)]$ complexes (L,L'-BID = monocharged bidentate ligand with donor atoms L and L'), formed by substituting one CO ligand in the parent $[\text{Rh}(\text{L},\text{L}'\text{-BID})(\text{CO})_2]$ complexes. In general, replacement of one CO ligand from a dicarbonyl complex containing an asymmetrical L,L'-BID ligand

may lead to the formation of two isomeric monocarbonyl complexes **A** and **B**:



If the difference in the donor/acceptor properties of the donor atoms L and L' is great enough, NMR studies of reaction mixtures revealed high selectivity of carbonyl group replacement: for instance, one isomer for 8-hydroxyquinolate [8] or two isomers with well-pronounced predominance of one of them for β -

* Corresponding authors.

¹ The authors dedicate their efforts to the memory of Professor Yuri Struchkov, who initiated X-ray study of rhodium(I) carbonylphosphine complexes of the type discussed in this publication.

aminovinylketonate ligands [6]. In these cases the sole (or predominant) isomer contains PPh_3 ligand in the trans-position to the more strong donor (less electronegative) atom, i.e. to nitrogen if O,N ligands are considered. If the donor capabilities of L and L' are close, isomers **A** and **B** are formed in comparable quantities. This is the case of complexes containing, for example, two donor oxygen atoms, asymmetrical β -diketonates, $[\text{Rh}(\text{R}_1\text{COCHCOR}_2)(\text{CO})(\text{PPh}_3)]$ with $\text{R}_1 \neq \text{R}_2$ [4].

Crystallographic studies on different of $[\text{Rh}(\text{L},\text{L}'\text{-BID})(\text{CO})(\text{PPh}_3)]$ complexes specifically revealed [1,2] that for the reaction between $[\text{Rh}(\text{L},\text{L}'\text{-BID})(\text{CO})_2]$ and PPh_3 , in most cases, only one isomer crystallizes from solution. However, the unique case where two isomers of the $[\text{Rh}(\text{BA})(\text{CO})(\text{PPh}_3)]$ complex (BA = benzoylacetonato) crystallized in the same unit cell was also noted [3].

We have shown previously that a good correlation between the Rh–P bond distance in the $[\text{Rh}(\text{L},\text{L}'\text{-BID})(\text{CO})(\text{PPh}_3)]$ complexes vs. donor/acceptor properties of the donor atom L' trans to the triphenylphosphine ligand exists [1,2]. Furthermore, a definite correlation between ring size and the Rh– PPh_3 bond distance has been observed, as well as a reasonable correlation between the Rh–CO bond distances, although limited data in this regard prevented significant conclusions [1].

NMR in these systems is an excellent technique for the identification of different isomers resulting from the reaction of $[\text{Rh}(\text{L},\text{L}'\text{-BID})(\text{CO})_2]$ with PPh_3 [4–9], since the nuclei are all of spin 1/2, with natural abundances of 100%, for ^{31}P and ^{103}Rh , and a high degree of ^{13}C enrichment is easily obtainable by direct ligand exchange. This enables accurate coupling constants to be determined, providing a unique opportunity by these ^{13}C and ^{31}P NMR studies to correlate the $^1J(^{31}\text{P}\text{-}^{103}\text{Rh})$ and $^1J(^{13}\text{C}\text{-}^{103}\text{Rh})$ values with the electron donating capability of the donor atom trans to the Rh–P and Rh–CO bonds [4–9] and the corresponding relationship with the respective bond lengths. We have extended this structural study to include the bond distance/donor

atom correlation with reactivity [2]. In this paper we extend this correlation further to include spin–spin coupling constants, the main contribution to which (on current interpretation) is due to the Fermi-contact interaction, the latter being principally dependent on the overlap of the valent s-orbitals [10].

2. Experimental

All manipulations were done under anaerobic conditions using analytical grade reagents.

2.1. Preparation of complexes. (Methyl 2-(amino)-1-cyclopentene-1-dithiocarboxylato- $\kappa\text{N},\kappa\text{S}$)-carbonyl(triphenylphosphine)rhodium(I), $[\text{Rh}(\text{hacsm})(\text{CO})(\text{PPh}_3)]$

The dicarbonyl complex, $[\text{Rh}(\text{hacsm})(\text{CO})_2]$, was first prepared, followed by the substitution of one carbonyl ligand by triphenylphosphine. $\text{RhCl}_3 \cdot 3\text{H}_2\text{O}$ (260 mg, ca. 1 mmol) was refluxed in DMF (20 ml) for ca. 30 min. Hhacsm ligand (170 mg, 1 mmol) was added to the cooled DMF solution followed by sodium acetate (ca. 500 mg). After precipitation by water (ca. 0°C) and centrifugation, a microcrystalline orange-brown product was obtained. To 5 ml of a cooled ether solution containing all of the $[\text{Rh}(\text{hacsm})(\text{CO})_2]$ product collected by centrifuge, PPh_3 (260 mg, ca. 1 mmol) was added, resulting in the immediate evolution of CO gas. After scratching the bottom of the beaker with a small spatula, the $[\text{Rh}(\text{hacsm})(\text{CO})(\text{PPh}_3)]$ complex precipitated as a microcrystalline product (400 mg, yield > 60%). IR (KBr, cm^{-1}): $\nu(\text{C} \equiv \text{O})$ 1965(s). Crystals suitable for the X-ray study of the $[\text{Rh}(\text{hacsm})(\text{CO})(\text{PPh}_3)]$ complex were obtained by slow evaporation (1–1.5 h) of a saturated acetone solution of the complex on ice. ^1H NMR(C_6D_6): δ 6.50 (b, 1H, N–H); 2.69 (s, 3H, S–CH₃); 1.69 (t, 2H, –CH₂₍₃₎); 1.29 (m, 2H, –CH₂₍₄₎); 2.91 (t, 2H, –CH₂₍₅₎); 7.75 (m, 6H, 2 (*m*-H–Ph)₃); 7.00 (m, 9H, 2 (*o*-H–Ph)₃ + 1 (*p*-H–Ph)₃).

Table 1
Crystallographic data for $[\text{Rh}(\text{hacsm})(\text{CO})(\text{PPh}_3)]$

Formula	$\text{C}_{26}\text{H}_{25}\text{NS}_2\text{OPRh}$	$\lambda(\text{Mo K}\alpha)$ (Å)	0.71073
Formula weight	565.47	V (Å ³)	2522.5(4)
Crystal system	Monoclinic	Z	4
Space group	$\text{P}2_1/c$	ρ_{calc} (g cm^{-3})	1.489
a (Å)	16.430(1)	T (K)	293
b (Å)	8.930(1)	μ (mm^{-1})	0.93
c (Å)	17.194(1)	Crystal dimensions (mm^3)	$0.30 \times 0.20 \times 0.12$
β (deg)	90.72(2)	No. unique reflections	3477
R (obs. reflns) ^a	0.0289	No. observed reflections ($F^2 > 3\sigma F^2$)	3143
R_w (obs. reflns) ^b	0.0721		

^a $R = (\sum |\Delta F|) / (\sum F_o)$.

^b $R_w = \{[\sum w(F_o^2 - F_c^2)^2] / [\sum w(F_o^2)^2]\}^{1/2}$; $w = [\sigma^2(F_o^2) + (0.030P)^2 + 2.0P]^{-1}$ with $P = [\max(F_o^2; 0) + 2F_c^2] / 3$.

2.2. Carbonylphosphinerhodium(I) complexes, $[Rh(L,L'-BID)(CO)(PPh_3)]$

The other $[Rh(L,L'-BID)(CO)(PPh_3)]$ complexes, with $L,L'-BID$ = monoanions of the following bidentate ligands: acac (acetylacetonate), Cupf (cupferronate), TTA (thenoyltrifluoroacetate), Sacac (thioacetylacetonate), HPT (1-hydroxy-2-pyridinethiolate), Ox (8-hydroxyquinolate), DMAVK (2-aminopenten-2-on-4-ate), AnMeTHA (4-hydroxy-*N*-methylbenzothiohydroxamate), TFAA (trifluoroacetylacetonate), Pic (2-pyridinecarboxylate), TROP (tropolonate), cacsm [(methyl 2-(cyclohexylamino)-1-cyclopentene-1-dithiocarboxylate)] and macsm [(methyl 2-(methylamino)-1-cyclopentene-1-dithiocarboxylate)] were prepared in a similar way as described for the $[Rh(hacsm)(CO)(PPh_3)]$ complex, as shown previously [1,2,4–9,11,12].

2.3. Alternative preparation of $[Rh(L,L'-BID)(CO)_2]$ complexes

These complexes can also be prepared by reacting $L,L'-BID$ ligand with $[Rh(CO)_2Cl]_2$ or $[Rh(AA)Cl]_2$

Table 2

Fractional atomic coordinates ($\times 10^4$) and equivalent isotropic thermal parameters ($\text{\AA}^2 \times 10^3$) for $[Rh(hacsm)(CO)(PPh_3)]$ with e.s.d. in parentheses

	<i>x</i>	<i>y</i>	<i>z</i>	U_{eq}^a
Rh	7938(1)	5979(1)	6166(1)	36(1)
P	6812(1)	4893(1)	6689(1)	34(1)
S(1)	9061(1)	7038(1)	5591(1)	54(1)
S(2)	10598(1)	8691(2)	5931(1)	93(1)
C(11)	6785(2)	2856(4)	6573(2)	37(1)
C(12)	6071(3)	2037(5)	6489(2)	48(1)
N	8237(2)	6906(4)	7202(2)	47(1)
O	7579(2)	4484(4)	4658(2)	81(1)
C(21)	5822(2)	5567(4)	6341(2)	38(1)
C(32)	7133(2)	4216(5)	8259(2)	48(1)
C(22)	5787(2)	6396(4)	5665(2)	45(1)
C(2)	8840(3)	7731(5)	7445(3)	52(1)
C(1)	7707(2)	5074(5)	5239(2)	48(1)
C(23)	5057(3)	6950(5)	5386(3)	63(1)
C(31)	6752(2)	5181(4)	7741(2)	39(1)
C(36)	6455(3)	6533(5)	8017(2)	54(1)
C(33)	7206(3)	4594(6)	9036(2)	64(1)
C(16)	7515(3)	2103(5)	6568(3)	54(1)
C(24)	4352(3)	6704(6)	5787(3)	71(2)
C(6)	9509(3)	8243(5)	7016(3)	59(1)
C(26)	5104(2)	5324(5)	6744(3)	55(1)
C(13)	6106(3)	488(5)	6411(3)	60(1)
C(7)	9660(2)	7966(5)	6250(3)	56(1)
C(35)	6534(3)	6901(6)	8796(3)	70(1)
C(3)	8908(4)	8269(7)	8275(3)	83(2)
C(25)	4376(3)	5889(6)	6462(3)	71(1)
C(15)	7541(3)	559(5)	6499(3)	63(1)
C(34)	6916(3)	5931(6)	9302(3)	71(1)
C(14)	6843(3)	-224(5)	6421(3)	61(1)
C(5)	10067(4)	9139(7)	7565(4)	96(2)
C(8)	10679(3)	8109(8)	4948(4)	107(2)

^a $U_{eq} = (1/3)\sum_i \sum_j U_{ij} a_i^* a_j^* (a_i a_j)$.

Table 3

Selected interatomic bond distances (Å) and angles (deg) for $[Rh(hacsm)(CO)(PPh_3)]$ with e.s.d. in parentheses

Rh–C(1)	1.823(4)	O–C(1)	1.148(5)
Rh–N	2.019(3)	C(2)–C(6)	1.408(6)
Rh–P	2.2827(10)	C(2)–C(3)	1.509(6)
Rh–S(1)	2.3074(11)	N–C(2)	1.299(5)
P–C(11)	1.830(4)	C(6)–C(7)	1.367(6)
S(1)–C(7)	1.707(5)	C(6)–C(5)	1.532(7)
S(2)–C(7)	1.764(4)	C(3)–C(4)	1.452(8)
S(2)–C(8)	1.776(7)	C(5)–C(4)	1.450(9)
C(1)–Rh–N	177.1(2)	C(6)–C(2)–C(3)	110.0(4)
C(1)–Rh–P	89.73(12)	O–C(1)–Rh	178.4(4)
N–Rh–P	90.98(11)	C(7)–C(6)–C(2)	126.8(4)
C(1)–Rh–S(1)	87.98(13)	C(7)–C(6)–C(5)	125.0(5)
N–Rh–S(1)	91.32(11)	C(2)–C(6)–C(5)	108.2(5)
P–Rh–S(1)	177.70(4)	C(6)–C(7)–S(1)	128.2(3)
C(7)–S(1)–Rh	111.8(2)	C(6)–C(7)–S(2)	113.7(3)
C(7)–S(2)–C(8)	105.4(3)	S(1)–C(7)–S(2)	118.1(3)
C(2)–N–Rh	133.9(3)	C(4)–C(3)–C(2)	104.0(5)
N–C(2)–C(6)	127.8(4)	C(4)–C(5)–C(6)	104.0(5)
N–C(2)–C(3)	122.2(4)	C(3)–C(4)–C(5)	111.8(6)

(AA = cyclooctadiene or norbornadiene) followed in the latter case by the bubbling of carbon monoxide through a solution of the intermediate $[Rh(L,L'-BID)(AA)]$ complex [4–9,13].

2.4. Structure

A summary of the general crystal data and refinement parameters for the $[Rh(hacsm)(CO)(PPh_3)]$ complex is given in Table 1. The fractional atomic coordinates and interatomic bond distances are reported in Tables 2 and 3 respectively. The structure was solved by the heavy-atom method using SHELXS86 [14], while SHELXL93 [15] was used for full-matrix least squares refinement on all non-hydrogen atoms. Hydrogen atom positions were calculated as riding on the adjacent carbon with C–H distances: phenyl C–H = 0.92 Å and

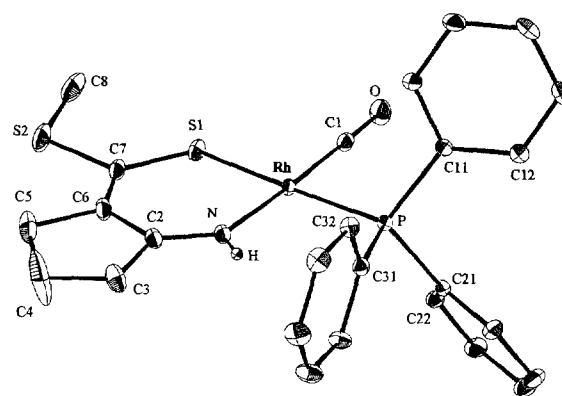


Fig. 1. Perspective view and atom numbering scheme of $[Rh(hacsm)(CO)(PPh_3)]$. The phenyl rings are numbered sequentially: the first digit is the ring number, and the second digit is the atom in the ring.

Table 4

Comparison of structural parameters in $[\text{Rh}(\text{L},\text{L}'\text{-BID})(\text{CO})(\text{PPh}_3)]$ complexes containing the aminocyclopentenedithiocarboxylato backbone (numbering scheme as in Fig. 1)

Parameter		macsm ^a	cacsm ^a	hacsm ^b
	PPh ₃ trans to CO trans to	N S	N S	S N
Bond distances to Rh (Å)	Rh–P	2.269(1)	2.268(1)	2.283(1)
	Rh–N	2.087(4)	2.125(3)	2.019(3)
	Rh–CO	1.836(5)	1.829(5)	1.823(4)
	Rh–S	2.298(1)	2.292(1)	2.307(1)
Bond distances in chelate ring (Å)	N–C(2)	1.305(6)	1.315(5)	1.299(6)
	C(2)–C(6)	1.434(8)	1.434(6)	1.408(6)
	C(6)–C(7)	1.367(7)	1.349(6)	1.367(6)
	C(7)–S(1)	1.713(5)	1.710(5)	1.707(5)
Bond angles (deg)	Bite angle	93.8(1)	93.5(1)	91.3(1)
	S(1)–Rh–P	87.5 (1)	85.6 (1)	177.7 (4)
	N(1)–Rh–C	94.1 (2)	97.8 (2)	177.1 (2)

^a Ref. [2]; ^b this study.

methylene C–H = 0.97 Å, and refined with an overall isotropic temperature factor. The position of the amino proton, H (Fig. 1), was obtained from a difference Fourier map. A complete list of bond lengths and angles and tables of thermal factors and hydrogen atom coordinates has been deposited at the Cambridge Crystallographic Data Centre.

2.5. NMR measurements

¹H, ¹³C and ³¹P NMR spectra were recorded on samples of the $[\text{Rh}(\text{L},\text{L}'\text{-BID})(\text{CO})(\text{PPh}_3)]$ complexes in CDCl₃ or C₆D₆ on a Bruker AM-500 spectrometer operating at 500.14 Hz, 125.76 Hz and 202.46 Hz respectively. The solvent resonances served as internal standards for ¹H and ¹³C spectra in CDCl₃ (δ ¹H = 7.25 ppm, δ ¹³C = 77.04 ppm), with 85% phosphoric acid (δ ³¹P = 0.0 ppm) as external standard for the ³¹P spectra. ¹³C NMR spectra were obtained using the ¹³CO-enriched complexes prepared by exchange with 50–75% enriched carbon monoxide [16] or from ¹³C-enriched $[\text{Rh}(\text{CO})_2\text{Cl}]_2$ [9]. Unless otherwise stated, all

coupling constants between the ¹⁰³Rh, ³¹P and ¹³C nuclei, e.g. ¹J(³¹P–¹⁰³Rh) and ¹J(¹³C–¹⁰³Rh), are denoted by ¹J(PRh) and ¹J(CRh) for simplicity.

2.6. IR measurements

IR spectra were recorded in KBr disks or chloroform solutions on a Hitachi 270-50 instrument.

3. Results

3.1. Structure

The $[\text{Rh}(\text{hacsm})(\text{CO})(\text{PPh}_3)]$ complex crystallizes as molecular moieties, of which the numbering scheme is given in Fig. 1. The distinct trans S–Rh–PPh₃ orientation is obvious. The structure of the $[\text{Rh}(\text{hacsm})(\text{CO})(\text{PPh}_3)]$ complex is similar to the two previously studied $[\text{Rh}(\text{N},\text{S}\text{-BID})(\text{CO})(\text{PPh}_3)]$ complexes, (N,S–BID = macsm and cacsm), with the important exception that in the aforementioned two struc-

Table 5

Average Rh–P and Rh–CO bond distances in complexes of the type $[\text{Rh}(\text{L},\text{L}'\text{-BID})(\text{CO})(\text{PPh}_3)]$ [1,17,11,12]

Donor atom trans to Rh–X ^a bond	Rh–P bond distance (Å)		Rh–CO bond distance (Å)	
	Five-membered chelate ring	Six-membered chelate ring	Five-membered chelate ring	Six-membered chelate ring
O	2.232	2.243	1.796	1.796
N	2.260	2.278	— ^b	1.823 ^c
S	2.281	2.300	1.82 ^d	1.833 ^e

^a X = P or CO; ^b not available; ^c this study; ^d Ref. [18]; ^e Ref. [2].

Table 6

Rh–P bond distances and NMR parameters of $[\text{Rh}(\text{L},\text{L}'\text{-BID})(\text{CO})(\text{PPh}_3)]$ complexes ^a from this study ^b, with L,L'-BID asymmetric unless otherwise indicated

No	Ligand	Reference	L ^c	L'	Ring size	Rh–P distance (Å)	$\delta^{31}\text{P}$ (ppm)	$^1J(\text{PRh})$ (Hz)	$\delta^{13}\text{C}$ (ppm)	$^1J(\text{CRh})$ (Hz)	$^2J(\text{CP})$ (Hz)
1	TFAA ^f	[1]	O	O	6	2.231(3)	47.72	176.9	188.24	77.6	24.6
2	TROP ^d	[1]	O	O	5	2.232(2)	49.57	177.7	188.18	77.4	24.8
3	Cupf	[1]	O	O	5	2.232(2)	48.85	171.1	189.90	76.7	25.4
4	acac ^d	[1]	O	O	6	2.244(4)	48.56	175.1	189.75	76.0	25.5
5	TTA	[1]	O	O	6	2.245(2)	47.84	177.7	188.12	77.8	24.6
6	Ox	[1]	N	O	5	2.261(2)	47.78	176.7	188.27	78.5	24.4
7	Pic	[1]	N	O	5	2.262(2)	41.40	161.6	190.70	72.3	22.6
8	cacsm	[2]	N	S	6	2.268(1)	40.24	161.9	189.84	75.3	22.5
9	DMAVK	[4–9,11]	N	O	6	2.275(1)	45.2	144.6	190.02	72.1	21.8
10	HPT	[18]	N	O	6	2.275(1)	41.45	149.7	191.20	73.8	21.9
11	hacsm	— ^e	S	N	6	2.278(1)	54.91	172.0	190.30	66.9	22.8
12	AnMeTHA ^g	[19]	S	O	5	2.283(1)	37.77	157.1	192.50	70.8	20.9
13	Sacac	[12]	S	O	6	2.290(1)	42.70	148.9	192.22	63.8	20.5
						2.300(2)	35.36	144.5	190.83	73.6	21.1

^a Data for predominant isomer are given in first row. ^b Although other complexes are known [19], only those investigated in this study are included. ^c L atom trans to atom P. ^d Symmetric O,O-BID ligand. ^e This study. ^f Rh–P distance for P(*p*-ClPh)₃ complex. ^g Rh–P distance for PCy₃ complex.

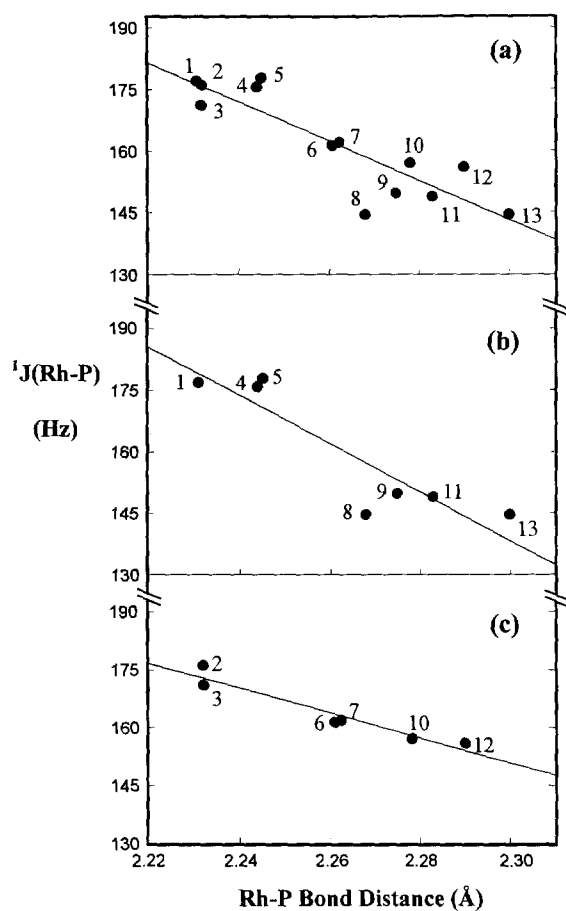


Fig. 2. Correlation between $^1J(\text{PRh})$ coupling constant (CDCl_3 , ambient temperature) and Rh–P bond distance in (a) all studied $[\text{Rh}(\text{L},\text{L}'\text{-BID})(\text{CO})(\text{PPh}_3)]$ complexes; (b) six-membered L,L'-BID chelate rings and (c) five-membered L,L'-BID chelate rings. The numbering of the complexes corresponds to that given in Table 6.

tures [2], the unique isomer obtained in solution (and crystallographically characterized) was that with a trans-N–Rh–PPh₃ orientation, rather than the trans-S–Rh–PPh₃ orientation found in this study (Fig. 1). Structural parameters of rhodium(I) complexes containing N,S-BID ligands are presented in Tables 4 and 5 and are discussed below.

3.2. ^{31}P and ^{13}C NMR data

In general, the NMR spectra of the solution containing two isomeric $[\text{Rh}(\text{L},\text{L}'\text{-BID})(\text{CO})(\text{PPh}_3)]$ complexes are as follows: (i) ^{31}P , two doublets with similar values of $\delta^{31}\text{P}$ and $^1J(\text{PRh})$ corresponding to the isomers A

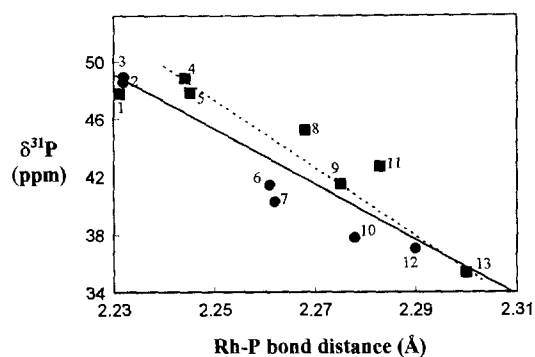


Fig. 3. Correlation between chemical shift $\delta^{31}\text{P}$ (CDCl_3 , ambient temperature) and Rh–P bond distance in all studied $[\text{Rh}(\text{L},\text{L}'\text{-BID})(\text{CO})(\text{PPh}_3)]$ complexes (—) and closely related $[\text{Rh}(\text{CH}_3\text{COCHXCH}_3)(\text{CO})(\text{PPh}_3)]$ complexes with X = O, NH, S (⋯): ■, six-membered L,L'-BID chelate rings; ●, five-membered L,L'-BID chelate rings. The numbering of the complexes corresponds to that given in Table 6.

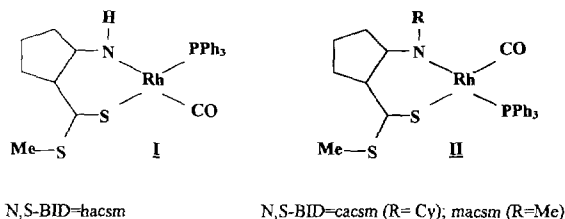
and **B** and (ii) ^{13}C , two doublets of doublets with similar values of $\delta^{13}\text{C}$, $^1J(\text{CRh})$, and $^2J(\text{CP})$ corresponding to the same isomers.

The ^{31}P and ^{13}C NMR data together with Rh–P bond distances for a range of $[\text{Rh}(\text{L},\text{L}'\text{-BID})(\text{CO})(\text{PPh}_3)]$ complexes, L,L'-BID = O,O'-BID (TROP, Cupf, acac, TFAA, TTA), O,N'-BID (Ox, DMAVK, Pic), O,S'-BID (HPT, AnMeTHA; Sacac), N,S'-BID (cacsm, hacsm) are summarized in Table 6 and are discussed in terms of the correlation between coupling constants ($^1J(\text{PRh})$ and $^1J(\text{CRh})$) and Rh–P and Rh–CO bond distances. The correlation between ^{31}P NMR parameters and Rh–P bond distances are also illustrated in Figs. 2 and 3.

4. Discussion

4.1. Specific isomer formation

Previous studies [1,20] showed that the structural trans effect (STE) for oxygen, nitrogen and sulphur follows the reverse electronegativity range, i.e. $\text{S} > \text{N} > \text{O}$. Thus, upon commencement of the study of the Rh(I) systems with N,S'-BID ligands, it was anticipated that the sole (or predominant) isomer of $[\text{Rh}(\text{N},\text{S}'\text{-BID})(\text{CO})(\text{PPh}_3)]$ formed in the reaction between the $[\text{Rh}(\text{N},\text{S}'\text{-BID})(\text{CO})_2]$ and PPh_3 would contain the phosphine ligand in the trans-position to the donor atom with the largest STE (i.e. sulphur). This expected substitution pattern is observed in the case of hacsm (see Fig. 1; **I** below).



The opposite substitution pattern was, however, observed in the $[\text{Rh}(\text{macsm})(\text{CO})(\text{PPh}_3)]$ and $[\text{Rh}(\text{cacsm})(\text{CO})(\text{PPh}_3)]$ complexes [2], i.e. the CO ligand trans to the nitrogen atom was substituted (see **II**). This unexpected substitution mode in these complexes was attributed to the much larger steric demand of the methyl and cyclohexyl groups on the nitrogen atom in the macsm and cacsm ligands respectively. It was, furthermore, concluded that the substitution mode observed in the $[\text{Rh}(\text{macsm})(\text{CO})(\text{PPh}_3)]$ and $[\text{Rh}(\text{cacsm})(\text{CO})(\text{PPh}_3)]$ complexes was sterically rather than electronically controlled. In the current study, we have specifically introduced the same aminocyclop-

tenedithiocarboxylato backbone used in the macsm and cacsm complexes, but have used a proton substituent on the amino N atom, rather than the more bulky methyl or cyclohexyl groups, to test the above hypothesis. It is clear from Fig. 1 that we have indeed succeeded in overriding the steric demand of the methyl or cyclohexyl substituents, forming primarily the trans-S–Rh–PPh₃ moiety. In this $[\text{Rh}(\text{hacsm})(\text{CO})(\text{PPh}_3)]$ complex the steric demand of the hydrogen atom as substituent on the nitrogen atom is negligible (Fig. 1) compared with that of the aforementioned groups, i.e. $-\text{CH}_3$ and $-\text{C}_6\text{H}_{11}$ [2], and the structure of the isomer formed is determined by the electronic influence.

4.2. Comparison of three $[\text{Rh}(\text{N},\text{S}'\text{-BID})(\text{CO})(\text{PPh}_3)]$ structures

The selected structural parameters of these three different $[\text{Rh}(\text{N},\text{S}'\text{-BID})(\text{CO})(\text{PPh}_3)]$ complexes, containing the macsm, cacsm and hacsm ligands, are summarized in Table 4. The N–Rh–S bite angles for the three complexes compare well with each other and are all in good agreement with the bite angle of ca. 90° expected for six-membered chelate rings, which allows for good overlap between the dsp^2 -orbitals of the metal and the orbitals of the bidentate ligand. The fact that in the case of hacsm the bite angle is the closest to the theoretical value of 90° is not unexpected, since the proton on the N donor atom will have a small steric interaction with the rest of the molecule (compared with $-\text{CH}_3$ or $-\text{C}_6\text{H}_{11}$) and will therefore have the smallest influence.

The Rh–P bond distance increases significantly from macsm and cacsm (P atom is trans to nitrogen), to hacsm (P trans to S), in agreement with the larger STE of sulphur compared with nitrogen.

The Rh–S bond distances, as might be expected, are comparable for macsm and cacsm (2.298(1) and 2.292(1) Å) [2], and both smaller than 2.307(1) Å in hacsm where the S-atom is trans to PPh₃, and not trans to a CO ligand as in macsm and cacsm. The Rh–N bond distance in $[\text{Rh}(\text{hacsm})(\text{CO})(\text{PPh}_3)]$ of 2.019(3) Å is much shorter than in the macsm and cacsm cases, since in the hacsm case the N donor atom is trans to a CO ligand of which the STE is smaller than that of PPh₃. The Rh–N distance of 2.087(4) Å for macsm, however, compares well with the observed distances of 2.088(6), 2.092(7), 2.098(9) and 2.045(4) Å in related $[\text{Rh}(\text{L},\text{L}'\text{-BID})(\text{CO})(\text{PPh}_3)]$ complexes containing nitrogen donor atoms in the bidentate ligands (L,L'-BID = 2-picolinate [21], *N*-*o*-tolylsalicylaldiminate [22], 8-hydroxyquinolate [23], and 2-aminovinylketonate [17] respectively). It is interesting to note the significant increase in the Rh–N bond distance of 2.125(3) Å in the case of cacsm, compared with that in macsm, i.e. 2.087(4) Å (Table 4). This, despite the comparable bite

angle of $93.5(1)^\circ$ that should allow for good overlap, as pointed out in above. The steric interaction between the bulky cyclohexyl group on the nitrogen atom and the carbonyl ligand caused the cacs m ligand to rotate away from the metal (yet still stay in the square plane) on the nitrogen side of the ligand and rotate toward the metal on the sulphur side; this is manifested in a shorter Rh–S bond distance of $2.292(1)$ compared with the equivalent bond distance of $2.298(1)$ Å in the macsm system. This shift of the *N,S*-BID ligand within the square plane was also observed in the respective decrease and increase of the S(1)–Rh–P and N(1)–Rh–C(1) angles ($85.6(1)^\circ$ and $97.8(2)^\circ$, Table 4) compared with the angles of $87.5(1)^\circ$ and $94.1(2)^\circ$ (S(1)–Rh–P and N–Rh–CO respectively) in the macsm complex, where the methyl group on the nitrogen atom will obviously have much less steric interaction with the adjacent carbonyl group. The net result of the large steric demand of the cyclohexyl group is therefore that the complete N–S bidentate backbone is ‘rotated’ in the plane, away from the Rh–CO direction toward the Rh–P bond by ca. $2\text{--}3^\circ$.

4.3. Correlation of structural data in $[\text{Rh}(\text{L},\text{L}'\text{-BID})(\text{CO})(\text{PPh}_3)]$ complexes

It was shown previously [1] that the Rh–P bond distance in square planar complexes of the type $[\text{Rh}(\text{L},\text{L}'\text{-BID})(\text{CO})(\text{PPh}_3)]$ is a good indicator of the relative STE of the donor atoms in the bidentate ligand (L,L'-BID), as summarized in Table 5. The Rh–P bond lengths found in the complexes with coordinated *N,S*-BID ligands, as discussed above, nicely fit in the expected range when compared with the average Rh–P bond lengths in these types of complex (Table 5), i.e. for oxygen, nitrogen and sulphur donor atoms [1,17,11,12] trans to the coordinated triphenylphosphine in five- and six-membered chelate ring systems.

The Rh–CO bond distances follow the same trend as the corresponding Rh–PPh₃ bonds, in good agreement with the STE for O, N and S as trans atoms observed from the Rh–P bond distance as discussed above (Table 5). In the $[\text{Rh}(\text{macsm})(\text{CO})(\text{PPh}_3)]$ and $[\text{Rh}(\text{cacs m})(\text{CO})(\text{PPh}_3)]$ complexes the Rh–CO bond lengths, of $1.836(5)$ Å and $1.829(5)$ Å respectively, correspond well to one another, the CO ligand being trans to a sulphur atom in both cases. However, in this situation the Rh–CO bond distances are significantly longer than in similar $[\text{Rh}(\text{L},\text{L}'\text{-BID})(\text{CO})(\text{PPh}_3)]$ complexes where the carbonyl was coordinated trans to an oxygen atom. In fact, the Rh–CO bond distance in 14 of these are comparable, with the average being $1.796(8)$ Å [1,17,11,20,12]. The Rh–CO bond lengthening in the trans-S–Rh–CO moieties (macsm and cacs m) can be directly attributed to the large STE of sulphur, increasing the nucleophilicity of the metal centre, thus

effectively decreasing the σ -donating ability of the CO ligand. The Rh–CO bond distance of $1.823(4)$ Å in the $[\text{Rh}(\text{hacs m})(\text{CO})(\text{PPh}_3)]$ complex, wherein the CO moiety is trans to a nitrogen atom, is of the expected magnitude (in the range $1.796(8)$ Å (for trans-O–Rh–CO moieties) to $1.833(5)$ Å (for trans-S–Rh–CO moieties)) [2].

Although the bond between Rh and the carbonyl ligand in macsm and cacs m complexes is lengthened, the increased nucleophilicity, and thus higher electron density of the Rh metal centre, can still influence the carbonyl group by donation of electron density from the metal to the π^* -orbitals of the carbonyl, decreasing the bonding order in the CO moiety. The observed stretching CO frequencies are 1944 cm^{-1} and 1956 cm^{-1} for the $[\text{Rh}(\text{cacs m})(\text{CO})(\text{PPh}_3)]$ and $[\text{Rh}(\text{macsm})(\text{CO})(\text{PPh}_3)]$ complexes respectively. Both these $\nu(\text{CO})$ values are smaller than the values of $1975\text{--}2000\text{ cm}^{-1}$ characteristic for trans-O–Rh–CO moieties in related complexes, supporting the argument above. The $\nu(\text{CO})$ value of 1965 cm^{-1} for $[\text{Rh}(\text{hacs m})(\text{CO})(\text{PPh}_3)]$, intermediate between the carbonyl stretching frequencies of the trans-O–Rh–CO and trans-S–Rh–CO moieties, corresponds to the range of increasing electron donating capability and STE: $\text{O} < \text{N} < \text{S}$.

4.4. Rh–P and Rh–C bond distances vs. $^1J(\text{PRh})$ and $^1J(\text{CRh})$

An earlier NMR study of $[\text{Rh}(\text{DMAVK})(\text{CO})(\text{PPh}_3)]$ (*N,O*-BID ligand) showed that as the σ -donor ability of the donor atom trans to a Rh–P bond increased, the value of $^1J(\text{PRh})$ decreased [6]. This observation is manifested in the trend that $^1J(\text{PRh}) = 149.7\text{ Hz}$ (P trans to N) is smaller than the $^1J(\text{PRh})$ value of 172.0 Hz (P trans to O) observed for the two isomers of the $[\text{Rh}(\text{DMAVK})(\text{CO})(\text{PPh}_3)]$ complex, for the predominant of which (P trans to N) an Rh–P bond length is given in Table 6. (The value of 172.0 Hz for $^1J(\text{PRh})$ (minor isomer with P trans to O) correlates well with the $^1J(\text{PRh})$ data ($171.1\text{--}177.8\text{ Hz}$ for entries 1–5 in Table 6) for complexes of this study with a similar P trans to O configuration.) This observation may be explained in terms of the increase in Rh–P bond distance expected for a trans-N–Rh–P orientation compared with an Rh–P bond distance in a trans-O–Rh–P moiety. In fact, the Rh–P bond distance of $2.275(1)$ Å is in excellent agreement with the data of average bond distances in Table 5 and is of the expected magnitude, i.e. between $2.243(2)\text{--}2.300(2)$ Å for the average bond distances of an Rh–P bond trans to O and S respectively, in six-membered chelate rings.

The data of Table 6 allow evaluation of the aforementioned observation, i.e. the greater the σ -donating ability (larger STE) of the atom trans to the Rh–P bond (causing elongation of the Rh–P bond), the lower the

$^1J(\text{PRh})$ value, as a result of less effective overlap of the $5s(\text{Rh})-3s(\text{P})$ orbitals. Investigation of the data in Table 6 shows that this trend generally holds, as can further be visualized in Fig. 2 where a plot of $^1J(\text{PRh})$ vs. Rh–P bond distance is shown. Although the general trend can be observed, the plot is not too convincing in terms of a possible linear relationship between the two parameters, especially noting the entry 8 for $[\text{Rh}(\text{cacsm})(\text{CO})(\text{PPh}_3)]$. (The fact of a linear relationship is in any case debatable considering the theory of spin–spin coupling [10].)

It was illustrated previously that the Rh–P bond distance in an $[\text{Rh}(\text{L},\text{L}'\text{-BID})(\text{CO})(\text{PR}_3)]$ complex depends on not only the nature of the donor atom (i.e. O, N or S) in the bidentate ligand, but also on the bite angle of the chelate ring. Thus, a separate presentation was done in an attempt to better resolve the crude correlation seen in Fig. 2(a). In Fig. 2(b) and Fig. 2(c) the $^1J(\text{PRh})$ values of complexes containing six- or five-membered chelate rings are plotted separately. It seems that the correlation for the five-membered chelates (Fig. 2(c)) is better than for the six-membered chelates (Fig. 2(b)). The data point plotted for the $[\text{Rh}(\text{cacsm})(\text{CO})(\text{PPh}_3)]$ (8) again shows the largest deviation from a general linear trend. This may be a consequence of a large solvent interaction with the latter complex. The $^1J(\text{PRh})$ value of 144.6 Hz is comparable with the 144.5 Hz for Sacac wherein the Rh–P distance is very long, i.e. 2.300(2) Å. Thus, it seems that the Rh–P bond in the $[\text{Rh}(\text{cacsm})(\text{CO})(\text{PPh}_3)]$ complex is substantially lengthened in solution by solvent interaction.

The $^1J(\text{CRh})$ values for $[\text{Rh}(\text{L},\text{L}'\text{-BID})(\text{CO})(\text{PR}_3)]$

complexes having the carbonyl ligand trans to an oxygen donor atom of the bidentate ligand (complexes 1–7, 9, 10, 12, 13, Table 6) are very similar; the average value for those mentioned is 74.8 Hz. In the complexes $[\text{Rh}(\text{hacsm})(\text{CO})(\text{PPh}_3)]$ and $[\text{Rh}(\text{DMAVK})(\text{CO})(\text{PPh}_3)]$ (minor isomer) the carbonyl ligand is trans to a nitrogen atom, and the decrease in the $^1J(\text{CRh})$ values, to 63.8 and 66.9 Hz respectively, is quite obvious (Table 6). This tendency corresponds to the longer Rh–CO bond distance of 1.823(4) Å (hacsm) compared with the average of 1.796(8) Å for the complexes in which the CO ligand is trans to an oxygen atom. It seems that the deviation of the $[\text{Rh}(\text{cacsm})(\text{CO})(\text{PPh}_3)]$ complex in terms of the correlation of Rh–P bond distance to the $^1J(\text{PRh})$ value mentioned earlier, repeats itself for the $^1J(\text{CRh})$ value (Table 7). In the latter complex the CO ligand is trans to a sulphur atom and the Rh–CO bond distance is 1.829(5) Å. It is therefore expected that a $^1J(\text{CRh})$ value close to those observed in the hacsm and DMAVK cases (63.8 and 66.9 Hz respectively) should be obtained, but definitely not such a large value as 72.1 Hz. This increase in the $^1J(\text{CRh})$ value is presumably caused by the Rh–C bond shortening in solution due to solvent interaction.

An interesting observation related to this NMR result is the fact that the change in $\nu(\text{C}\equiv\text{O})$ for the latter cacsm complex in a KBr-disk to CHCl_3 solution is 50 cm^{-1} , confirming substantial solvent interaction ($\nu(\text{C}\equiv\text{O})\text{ cm}^{-1}$: 1944 (KBr), 1994 (CHCl_3)). The change in $\nu(\text{C}\equiv\text{O})$ in the case of DMAVK and acac is only 4 cm^{-1} and ca. 0 cm^{-1} respectively ($\nu(\text{C}\equiv\text{O})\text{ cm}^{-1}$: DMAVK: 1960 (KBr), 1964 (CHCl_3); acac: 1983 (KBr), 1983 (CHCl_3)). A further interesting obser-

Table 7
NMR parameters and Rh–P and Rh–CO bond distances for selected complexes of the type $[\text{Rh}(\text{L},\text{L}'\text{-BID})(\text{CO})(\text{PPh}_3)]$ and $[\text{Rh}(\text{L},\text{L}'\text{-BID})(\text{CO})_2]$

Bond Rh–X ^a	Trans bond L–Rh–X ^a	L,L'–BID	$^1J(\text{XRh}^a)$ (Hz)	Rh–X ^a bond distance (Å)	
Rh–CO	O–Rh–CO	acac ^b	73.0	—	
		DMAVK ^b	70.9	—	
		acac ^c	75.7	1.801(8)	
		DMAVK ^c	73.8	1.784(5)	
		Sacac ^c	73.6	1.808(2)	
		N–Rh–CO	DMAVK ^b	64.1	—
		DMAVK ^c	66.9	—	
		hacsm ^c	63.8	1.823(4)	
		S–Rh–CO	cacsm ^c	72.1	1.829(5)
	Rh–P	O–Rh–P	acac ^c	175.7	2.244(2)
DMAVK ^c			172.0	—	
N–Rh–P		DMAVK ^c	149.7	2.275(1)	
			cacsm ^c	144.6	2.268(1)
S–Rh–P		hacsm ^c	148.9	2.283(1)	
		Sacac ^c	144.5	2.300(2)	

^a X = P or CO; ^b in $[\text{Rh}(\text{L},\text{L}'\text{-BID})(\text{CO})_2]$ complex; ^c in $[\text{Rh}(\text{L},\text{L}'\text{-BID})(\text{CO})(\text{PPh}_3)]$ complex.

vation is the fact that the $[\text{Rh}(\text{cacsm})(\text{CO})(\text{PPh}_3)]$ complex crystallized from solution as an adduct with a solvent molecule (acetone) [2].

4.5. Rh–P bond distance vs. $\delta^{31}\text{P}$

The correlation between the chemical shift ($\delta^{31}\text{P}$) vs. Rh–P bond distance is presented on Fig. 3. Since the chemical shift is dependent on many factors, it is to be expected that this parameter, for the range of complexes studied, should not necessarily vary in parallel with the Rh–P bond distance. It is therefore not discussed further, although it is interesting to note that the data points plotted for the six-membered chelates tend to be above the arbitrary straight line for a hypothetical linear relationship, and the opposite is observed for the five-membered chelates. This observation, if indeed true in general, cannot be explained at this point. Note, however, that the points 4, 9, 13 for three similar $[\text{Rh}(\text{CH}_3\text{COCHXCH}_3)(\text{CO})(\text{PPh}_3)]$ complexes, with X = O, NH, S respectively, fall on a straight line ideally. Further research is currently being planned to specifically address the effect of different phosphine ligands in these systems in terms of basicity and steric demand, correlated with theoretical calculations and reactivity studies.

Acknowledgements

Financial assistance from the South African FRD and the University of the Orange Free State is gratefully acknowledged.

References

- [1] D.E. Graham, G.J. Lamprecht, I.M. Potgieter, A. Roodt and J.G. Leipoldt, *Transition Met. Chem.*, **16** (1991) 193.
- [2] (a) G.J.J. Steyn, A. Roodt and J.G. Leipoldt, *Inorg. Chem.*, **31** (1992) 3477 and references cited therein. (b) G.J.J. Steyn and A. Roodt, submitted to *Polyhedron*.
- [3] W. Purcell, S.S. Basson, J.G. Leipoldt, A. Roodt and P. Preston, *Inorg. Chim. Acta*, in press.
- [4] A.M. Trzeciak and J.J. Ziolkowski, *Inorg. Chim. Acta*, **96** (1985) 15.
- [5] T.G. Cherkasova, L.V. Osetrova and Yu.S. Varshavsky, *Rhodium Express*, **1** (1993) 8.
- [6] M.R. Galding, T.G. Cherkasova, L.V. Osetrova and Yu.S. Varshavsky, *Rhodium Express*, **1** (1993) 14.
- [7] I.A. Poletaeva, T.G. Cherkasova, L.V. Osetrova, Yu.S. Varshavsky, A. Roodt and J.G. Leipoldt, *Rhodium Express*, **3** (1994) 21.
- [8] Yu.S. Varshavsky, T.G. Cherkasova, N.A. Buzina and L.S. Bresler, *J. Organomet. Chem.*, **464** (1994) 239.
- [9] T.G. Cherkasova, Yu.S. Varshavsky, I.S. Podkorytov and L.V. Osetrova, *Rhodium Express*, **0** (1993) 21.
- [10] (a) J.A. Pople and D.P. Santry, *Mol. Phys.*, **8** (1964) 1. (b) J.F. Nixon and A. Pidcock, *Ann. Rev. NMR Spectrosc.*, **2** (1969) 346. (c) S. Otto, A. Roodt and J.G. Leipoldt, *S. Afr. Jour. Chem.*, in press.
- [11] S.S. Basson, J.G. Leipoldt, W. Purcell, G.J. Lamprecht and H. Preston, *Acta Crystallogr. Sect. C*, **48** (1992) 169.
- [12] (a) H. Preston, *Ph. D. Thesis*, University of the Orange Free State, Bloemfontein, South Africa, 1993. (b) S.S. Basson, J.G. Leipoldt, A. Roodt and H. Preston, *Acta Crystallogr. Sect. C*, **47** (1991) 1961.
- [13] J.V. Heras, E.P. Pinilla and M. Martinez, *Polyhedron*, **2** (1983) 1009.
- [14] G.M. Sheldrick, *Acta Crystallogr. Sect. A*, **46** (1990) 467.
- [15] G.M. Sheldrick, in preparation.
- [16] L.S. Bresler, N.A. Buzina, Yu.S. Varshavsky, N.V. Kiseleva and T.G. Cherkasova, *J. Organomet. Chem.*, **171** (1979) 229.
- [17] L.J. Damoense, W. Purcell, A. Roodt and J.G. Leipoldt, *Rhodium Express*, **5** (1994) 10.
- [18] G.J.J. Steyn and A. Roodt, in preparation.
- [19] (a) M. Cano, J.V. Heras, M.A. Lobo, E. Pinilla and M.A. Monge, *Polyhedron*, **13** (1994) 1563. (b) M. Cano, J.V. Heras, M.A. Lobo, P. Ovejera, J.A. Campo, E. Pinilla and M.A. Monge, *Rhodium Express*, **9** (1995) 8.
- [20] L.J. Botha, S.S. Basson and J.G. Leipoldt, *Inorg. Chim. Acta*, **126** (1987) 25.
- [21] J.G. Leipoldt, J.G. Lamprecht and D.E. Graham, *Inorg. Chim. Acta*, **101** (1985) 123.
- [22] J.G. Leipoldt, S.S. Basson, E.C. Grobler and A. Roodt, *Inorg. Chim. Acta*, **99** (1985) 13.
- [23] (a) J.G. Leipoldt, S.S. Basson and C.R. Dennis, *Inorg. Chim. Acta*, **50** (1981) 121. (b) L.G. Kuzmina, Yu.S. Varshavsky, N.G. Boky, Yu.T. Struchkov and T.G. Cherkasova, *Zh. Strukt. Khim. (Russ.)*, **12** (1971) 653.